

PDF hosted at the Radboud Repository of the Radboud University Nijmegen

The following full text is a publisher's version.

For additional information about this publication click this link.

<http://hdl.handle.net/2066/112832>

Please be advised that this information was generated on 2017-12-06 and may be subject to change.

One-dimensional subband effects in the conductance of multiple quantum wires in Si metal-oxide-semiconductor field-effect transistors

J. R. Gao, C. de Graaf, J. Caro, and S. Radelaar

*Delft Institute for Microelectronics and Submicron Technology, Delft University of Technology,
Lorentzweg 1, 2628 CJ Delft, The Netherlands*

M. Offenberg and V. Lauer

Institute of Semiconductor Electronics, Aachen Technical University, D-5100 Aachen, West Germany

J. Singleton, T. J. B. M. Janssen, and J. A. A. J. Perenboom

*High Field Magnet Laboratory, University of Nijmegen, Toernooiveld, 6525 ED Nijmegen, The Netherlands
(Received 26 January 1990; revised manuscript received 26 March 1990)*

The electrical transport in narrow (60–80 nm), parallel multiple quantum wires in Si metal-oxide-semiconductor field-effect transistors (MOSFET's) has been studied at 0.2 K as a function of gate voltage in zero magnetic field and in fields up to 20 T. The conductance of the multiple wires as a function of gate voltage shows well-resolved structures due to successive population of one-dimensional subbands. In addition, quantum oscillations in the gate-voltage derivative of the conductance as a function of magnetic field show, for the first time in a Si MOSFET, characteristics due to magnetic depopulation of one-dimensional subbands.

In a quasi-one-dimensional electron gas (quasi-1D EG), electrons are confined in two directions, while they move freely in the third direction. This confinement gives rise to discrete energy levels E_n and each of these levels is the bottom of a parabolic energy band associated with the direction of free motion (1D subbands). For an ideal system the density of states (DOS) of the n th 1D subband is a sharp peak that starts at energy E_n and falls off as $(E - E_n)^{-1/2}$. The total DOS is the sum of such functions, the peaks being separated by the subband spacing. Usually a 1D EG is obtained by lateral confinement of a two-dimensional electron gas (2D EG) in a Si metal-oxide-semiconductor field-effect transistor (MOSFET) or a GaAs-Al_xGa_{1-x}As heterostructure by means of mesa-etching or electrostatic confinement, thus creating a so-called quantum wire.

A major effect expected in a quantum wire is a modulation of the conductance as a function of Fermi energy, reflecting the peaks in the total DOS. Many efforts have already been made to study these 1D subbands in the conductance of Si MOSFET's,¹ but in devices with a single channel or a small number of channels their observation was obscured by universal conductance fluctuations² (UCF) that dominated the structure in the conductance. To overcome this problem Warren, Antoniadis, and Smith³ pioneered the use of a few hundred parallel inversion channels in a Si MOSFET to average out UCF. The idea is that 1D-subband effects, being coherent for identical channels, are not affected by the averaging. In such a device Warren *et al.* indeed observed a weak oscillatory component in the transconductance as a function of gate voltage. They believed this was a clear observation of the quasi one-dimensional density of states.

Recently, 1D-subband effects were also observed in multichannel Si MOS capacitors by far-infrared (FIR) spectroscopy.⁴ For narrow channels in III-V heterostruc-

tures, the quantization of electrons into 1D subbands has been observed by many authors, using electron-transport measurements,⁵⁻⁷ capacitance measurements,⁸ and FIR spectroscopy.^{9,10}

In this Rapid Communication we present experimental data on 1D-subband effects in the conductance of multiple, parallel quantum wires in Si MOSFET's. In our experiments, in contrast to those reported in Ref. 3, the conductance itself already shows well-resolved regular structures as a function of gate voltage. In addition, we measured quantum oscillations in the gate voltage derivative of the conductance of these devices in magnetic fields up to 20 T. The observed oscillations show clear characteristics due to magnetic depopulation of 1D subbands. Consequently, our quantum oscillation data, in conjunction with the gate-voltage dependence of the conductance, now give conclusive evidence for 1D-subband effects in the conductance of MOSFET quantum wires.

The devices used in the experiments are dual-gate Si MOSFET's with 240 parallel narrow channels. A magnified cross section of a device is shown in Fig. 1. The device is similar to that of Warren *et al.*,³ except for the grating-gate material and the insulator covering the grating gate, which in our devices are polysilicon and silicon nitride, respectively. Fabrication starts on *p*-type Si substrates with a resistivity of 20–30 Ω cm. After growth of a 25-nm-thick gate oxide and deposition of 80-nm n^+ polysilicon, grating gates were patterned by *e*-beam lithography and reactive-ion etching. The period of the gratings is 200 nm, with equal lines and spaces. Subsequently, 120-nm chemical-vapor-deposited silicon nitride was deposited as a second insulator. Finally aluminum was evaporated to form upper gates and electrical contacts.

By applying a positive voltage V_{GU} to the upper gate to create inversion, while simultaneously applying a negative voltage V_{GL} to the lower gate, conducting channels are

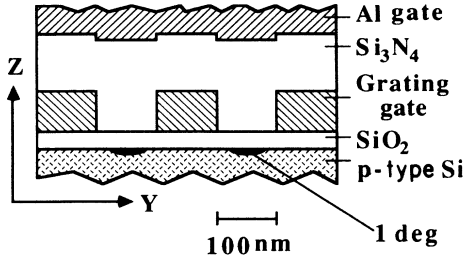


FIG. 1. Magnified cross section of a dual-gate Si MOSFET with 240 parallel grating lines operating in gap-confinement mode. The area of the multiple channels is $24 \times 48 \mu\text{m}^2$.

formed in the so-called gap-confinement mode, in which electrons are confined in the region under the gaps between the grating lines (see Fig. 1). In this mode inversion channels are substantially narrower than the width of the gap because of fringing fields contributing to the confining potential.

Measurements were done in two different ^3He - ^4He dilution refrigerators, one of these being placed within a 20-T Bitter magnet. By means of a low-frequency lock-in technique, we either measure the conductance at low-level source-drain voltage V_{DS} or measure the first derivative of the conductance $\partial G/\partial V_{GU}$ by modulating the upper gate voltage, in both cases at constant lower gate voltage.

We carried out measurements of the conductance of several identical quantum wire devices as a function of upper gate voltage. The conductance did not show UCF, indicating an effective averaging. Instead, a clear feature was observed that repeated itself at a number of gate voltages. Figure 2 shows an example of the measured conductance of device U3 as a function of V_{GU} at 0.2 K and zero magnetic field. In Fig. 2, six features are indicated by arrows. To determine the exact positions of the features, $\partial G/\partial V_{GU}$ was calculated by differentiation of a quadratic fit to conductance data within a window of width 0.6 V around each data point. As also shown in Fig. 2, the derivative $\partial G/\partial V_{GU}$ oscillates regularly. This directly reflects the nonuniform DOS of the quasi-1D EG and, as explained below, the local minima in the derivative correspond to values of the Fermi energy at which population of a new 1D subband starts.

By counting minima in $\partial G/\partial V_{GU}$ a plot of the subband index n vs V_{GU} can be constructed. The result is shown in the inset of Fig. 2 and the line is a linear fit to the data points. The point at $V_{GU} = 20$ V is designated as $n=1$ ($n=0$ denotes the ground state). This was deduced from the fact that threshold for conduction is clearly below 20 V. In fact, the threshold $V_{GU,T}$ could not be reliably determined due to the low conductance at the onset of conduction, but we estimate it to be 18.4 V. The 1D electron density can be approximated by $N_{1D} = WC(V_{GU} - V_{GU,T})/e$. Here W is the channel width and $C(V_{GU} - V_{GU,T})/e$ is the areal electron density. Using 70 nm (the width found from fitting the appropriate theoretical 1D expression¹¹ to low-field magnetoconductance (LFMC) data of device U4 taken around 6 V above threshold) as the channel width and a capacitance¹² of

$2.8 \times 10^{-8} \text{ F/cm}^2$, the 1D electron density at $V_{GU} = 20$ V due to the zeroth subband amounts to $2 \times 10^6 \text{ cm}^{-1}$. This value may be compared with the numerical results of Laux and Stern¹³ for a device structure very similar to ours. Their results indicate that the $n=1$ subband starts filling at $N_{1D} \approx 2.2 \times 10^6 \text{ cm}^{-1}$. Thus, our designation of the subband index is in agreement with this.

The spacing of successive minima in $\partial G/\partial V_{GU}$ is approximately constant and its average value ΔV_{GU} amounts to 1.1 V. It is now tempting to convert ΔV_{GU} to an energy spacing, using $N_{2D} = C(V_{GU} - V_{GU,T})/e = 2m^*E_F/\pi\hbar^2$ (in a 1D system there is no simple relation between V_{GU} and E_F , so we have to rely on the 2D approximation), and to designate it as $\hbar\omega_0$, the level spacing of a harmonic potential that seems to describe the confinement. Using $m^* = 0.19m_0$, this gives $\hbar\omega_0 = 1.2 \text{ meV}$, independent of V_{GU} . We compared this level spacing with the value given by $\hbar\omega_0 = 2\hbar(2E_F/m^*)^{1/2}/W_{\text{eff}}$, which follows from equating the harmonic potential for a distance $W_{\text{eff}}/2$ from the potential minimum to the Fermi energy. Using 70 nm, the above-mentioned width derived from LFMC experiments, as the effective width we found $\hbar\omega_0 = 2.1 \text{ meV}$, approximately consistent with $\hbar\omega_0 = 1.2 \text{ meV}$.

To discuss the observed structure in the conductance in more detail, several mechanisms that influence its shape should be taken into account. In a quasi-1D EG with weak elastic scattering, the conductance has a strong dip when a new subband is populated. This is due to enhanced scattering when a high density of final states becomes available. The dip can be smeared by level broadening induced by strong elastic scattering, by width variations inside a channel and among channels and by thermal broadening. Since the measurements described here were done at 0.2 K, to be compared with the subband spacing of 1.2 meV, thermal broadening plays no role here. Broadening due to elastic scattering, however, is substantial in our devices. This is indicated by a mobility

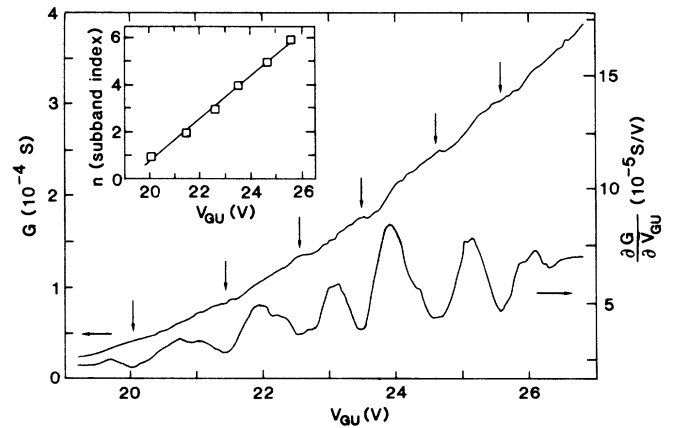


FIG. 2. Conductance G (left-hand scale) and derivative $\partial G/\partial V_{GU}$ (right-hand scale) of device U3 as a function of V_{GU} at 0.2 K and $B=0$. $V_{GL} = -0.3$ V and $V_{DS} = 17 \mu\text{V}$. At the position of the six features indicated by arrows the Fermi energy enters a new 1D subband. The inset shows a plot of the subband index n vs the position of the minima in $\partial G/\partial V_{GU}$. The line in the inset is a linear fit to the data points.

μ of $5000 \text{ cm}^2/\text{Vs}$, that was obtained from 2D MOSFET's fabricated on the same wafer. From this it follows that the level broadening defined as $\Gamma = \hbar/2\tau$, with τ given by $m^*\mu/e$, amounts to 0.6 meV . Calculations of DasSarma and Xie¹⁴ indicate that for a ratio of Γ to the subband spacing comparable to ours, the dip in the conductance develops into a local decrease of the slope of the conductance curve, in agreement with our data in Fig. 2. In principle variations in the width of the channels have the same effect as impurity broadening. Width variations of the grating lines in our devices as found from scanning electron microscopy are within 10%. We note that the criterion for observation of 1D-subband effects of DasSarma and Xie,¹⁴ who stated that $\Delta W/\bar{W}$ (\bar{W} is the average width) of a channel should be within 10–15%, is apparently adequate.

In a second type of experiment we have measured the dependence of $\partial G/\partial V_{\text{GU}}$ on a magnetic field directed perpendicular to the plane of the quantum wires. Derivative traces for device D1 were measured at four different V_{GU} and for magnetic fields up to 20 T. Each of these curves exhibited three or four oscillations and these were identified as quantum oscillations related to the Shubnikov-de Haas (SdH) effect. Starting at the highest field we counted the number of maxima in each curve using the index n . Figure 3 shows the result in a plot of the index n vs $1/B$. The inset in Fig. 3 shows measured oscillations at $V_{\text{GU}} = 27.5 \text{ V}$. The dashed lines are straight lines through $1/B = 0$ fitted to the lowest two data points in $1/B$. We note that for each V_{GU} a line connecting the lowest two data points would already extrapolate well to $1/B = 0$, as expected for a 2D EG. At higher $1/B$ values the dependence of n on $1/B$ departs from linearity. The overall behavior is characteristic of quantum oscillations in a 1D-subband system.^{5,6,15} In a magnetic field the subbands of

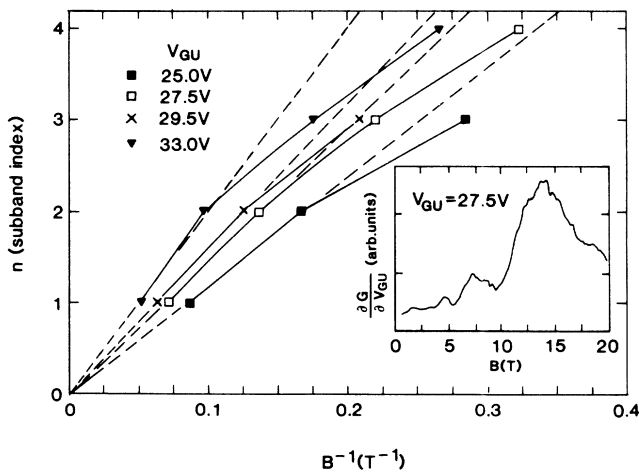


FIG. 3. Plot of subband index n vs $1/B$ deduced from oscillations in $\partial G/\partial V_{\text{GU}}(B)$ of device D1 at four values of V_{GU} . A pronounced deviation from a 2D behavior is indicated by the dashed lines. $T = 0.2 \text{ K}$, $V_{\text{GL}} = 0$, $V_{\text{DS}} = 0.5 \text{ mV}$, and the amplitude of the upper gate voltage modulation is 0.35 V . Inset: measured oscillations at $V_{\text{GU}} = 27.5 \text{ V}$.

such a system develop into hybrid magnetoelectric subbands. With increasing magnetic field the subband spacing increases, giving rise to magnetic depopulation. This phenomenon is reflected by the departure from linearity in the plot of Fig. 3. At high enough fields (where the cyclotron radius \ll the channel width) the subbands coincide with the Landau levels and the system is effectively a 2D EG. In Fig. 3 the slope of the dashed lines increases with increasing gate voltage (areal electron density), consistent with 2D EG behavior. To our knowledge a deviation from linearity of the n vs $1/B$ plot due to magnetic depopulation of 1D subbands in Si-MOSFET quantum wires has not been reported before.

Approximate values of E_F and the subband spacing $\hbar\omega_0$ can be found by assuming a harmonic potential $V(y) = m^*\omega_0^2 y^2/2$ for electrical confinement in the y direction. The hybrid subbands then have energies $E_n = (n + \frac{1}{2})\hbar\omega$, with $\omega^2 = \omega_0^2 + \omega_c^2$. Here $\omega_c = eB/m^*$ is the cyclotron frequency. Each oscillation maximum corresponds to a field at which $E_n = E_F$. For each V_{GU} , E_F and ω_0 were adjusted to fit the experimental positions of the maxima. The results are summarized in Table I, together with effective channel widths and electron densities. The effective channel width was obtained from the potential width at the Fermi energy that equals $W_{\text{eff}} = (8E_F/m^*\omega_0^2)^{1/2}$ and the electron density is given by $N_{1\text{D}} = W_{\text{eff}}N_{2\text{D}}$, with $N_{2\text{D}}$ as defined above.

In comparing the $\hbar\omega_0$ values in Table I with $\hbar\omega_0 = 1.2 \text{ meV}$, derived from the data in Fig. 2 we note a discrepancy. At present we cannot explain this, although uncertainties (capacitance of the double layer, comparison of results from different types of experiments on different devices) may play a role. The widths and electron densities in Table I are in accordance with a width of 70 nm as derived from the LFMC experiments and with an extrapolation of the electron densities calculated by Laux and Stern,¹³ respectively. Further, we notice a competition between E_F and $\hbar\omega_0$: with increasing E_F , $\hbar\omega_0$ also increases, making it harder to populate the next level. This still can be in qualitative agreement with the constant spacing of minima in Fig. 2, since possibly $\Delta V_{\text{GU}} = 1.1 \text{ V}$ between successive minima is used to raise the Fermi level from $(n + \frac{1}{2})\hbar\omega_{0,n}$ to $(n + \frac{3}{2})\hbar\omega_{0,n+1}$ ($\hbar\omega_{0,n+1} > \hbar\omega_{0,n}$). Although the quality of the fit is good, some care should be taken in interpreting the fitted parameters in Table I due to the assumption of a harmonic potential. The real potential may deviate from the parabolic shape

TABLE I. Parameters derived from the quantum oscillations in $\partial G/\partial V_{\text{GU}}(B)$. Listed quantities are Fermi energy E_F , subband spacing $\hbar\omega_0$, effective channel width W_{eff} , and electron density $N_{1\text{D}}$, as a function of the upper gate voltage V_{GU} .

$V_{\text{GU}}(\text{V})$	E_F (meV)	$\hbar\omega_0$ (meV)	W_{eff} (nm)	$N_{1\text{D}}$ (10^7 cm^{-2})
25.0	11.0	2.3	82	1.4
27.5	13.2	2.6	79	1.7
29.5	15.1	3.2	69	1.7
33.0	18.5	4.0	61	1.8

and (part of the) dependence of $\hbar\omega_0$ on V_{GU} that we found may be specific for the assumed model potential. It will be clear that further interpretation of our experimental data would benefit from a calculation of the real confinement potential and its dependence on both upper and lower gate voltage.

In summary, we have observed effects in the electrical transport in narrow (60–80 nm) multiple quantum wires in Si MOSFET's that unambiguously originate from 1D-subbands. The conductance as a function of Fermi energy shows well-resolved structures that reflect the subsequent filling of 1D subbands. Quantum oscillations in the gate-voltage derivative of the conductance as a function of magnetic field show, for the first time in a Si MOSFET, a

deviation from 2D SdH oscillations due to magnetic depopulation of 1D subbands.

The authors wish to express their gratitude to P. Balk, D. Laschet, A. H. Verbruggen, L. E. M. de Groot, and J. M. G. Teven for their contributions to this work and to H. M. Jäger, B. J. van Wees, and L. P. Kouwenhoven for helpful discussions. We thank the Solid State Physics Group of the Faculty of Applied Physics for the use of their dilution refrigerator. This work is part of the research program of the "Stichting voor Fundamenteel Onderzoek der Materie," which is financially supported by the "Nederlandse Organisatie voor Wetenschappelijk Onderzoek."

¹W. J. Skocpol, L. D. Jackel, R. E. Howard, P. M. Mankiewich, D. M. Tennant, A. E. White, and R. C. Dynes, *Surf. Sci.* **170**, 1 (1986), and references therein.

²P. A. Lee, A. D. Stone, and H. Fukuyama, *Phys. Rev. B* **35**, 1039 (1987). For recent experiments see J. R. Gao, J. Caro, A. H. Verbruggen, S. Radelaar, and J. Middelhoek, *Phys. Rev. B* **40**, 11 676 (1989).

³A. C. Warren, D. A. Antoniadis, and H. I. Smith, *Phys. Rev. Lett.* **56**, 1858 (1986).

⁴J. P. Kotthaus, W. Hansen, H. Pohlmann, M. Wassermeier, and K. Ploog, *Surf. Sci.* **196**, 600 (1988); and J. Alsmeier, E. Batke, and J. P. Kotthaus, *Phys. Rev. B* **40**, 12 574 (1989).

⁵K.-F. Berggren, T. J. Thornton, D. J. Newson, and M. Pepper, *Phys. Rev. Lett.* **57**, 1769 (1986).

⁶F. Brinkop, W. Hansen, J. P. Kotthaus, and K. Ploog, *Phys. Rev. B* **37**, 6547 (1988).

⁷K. Ismail, D. A. Antoniadis, and H. I. Smith, *Appl. Phys. Lett.* **54**, 1130 (1989).

⁸T. P. Smith III, H. Arnot, J. M. Hong, C. M. Knoedler, S. E. Laux, and H. Schmid, *Phys. Rev. Lett.* **59**, 2802 (1987).

⁹W. Hansen, M. Horst, J. P. Kotthaus, U. Merkt, Ch. Sikorski, and K. Ploog, *Phys. Rev. Lett.* **58**, 2586 (1987).

¹⁰J. Alsmeier, Ch. Sikorski, and U. Merkt, *Phys. Rev. B* **37**, 4314 (1988).

¹¹B. L. Al'tshuler and A. G. Aronov, *Pis'ma Zh. Eksp. Teor. Fiz.* **33**, 515 (1981) [*JETP Lett.* **33**, 499 (1981)].

¹²This figure was derived by taking into account that in the gaps about 5-nm gate oxide was consumed due to a slight overetch of the polysilicon and that the nitride thickness above the gaps, as found from SUPREM4 modeling (developed by Technology Modeling Associates, Inc.) amounts to 195 nm.

¹³S. E. Laux and F. Stern, *Appl. Phys. Lett.* **49**, 91 (1986).

¹⁴S. DasSarma and X. C. Xie, *Phys. Rev. B* **35**, 9875 (1987).

¹⁵S. B. Kaplan and A. C. Warren, *Phys. Rev. B* **34**, 1346 (1986).